ROYAL SOCIETY OF CHEMISTRY

EDGE ARTICLE

Check for updates

Self-healing and shape memory functions exhibited by supramolecular liquid-crystalline networks formed by combination of hydrogen bonding interactions and coordination bonding†

Junya Uchida, [ID] * Masafumi Yoshio‡ and Takashi Kato [ID] *

We here report a new approach to develop self-healing shape memory supramolecular liquid-crystalline (LC) networks through self-assembly of molecular building blocks *via* combination of hydrogen bonding and coordination bonding. We have designed and synthesized supramolecular LC polymers and networks based on the complexation of a forklike mesogenic ligand with Ag$^+$ ions and carboxylic acids. Unidirectionally aligned fibers and free-standing films forming layered LC nanostructures have been obtained for the supramolecular LC networks. We have found that hybrid supramolecular LC networks formed through metal–ligand interactions and hydrogen bonding exhibit both self-healing properties and shape memory functions, while hydrogen-bonded LC networks only show self-healing properties. The combination of hydrogen bonds and metal–ligand interactions allows the tuning of intermolecular interactions and self-assembled structures, leading to the formation of the dynamic supramolecular LC materials. The new material design presented here has potential for the development of smart LC materials and functional LC membranes with tunable responsiveness.

Introduction

Nanostructured liquid crystals have attracted attention because of great potential as new functional materials.[1–10] In particular, combination of nano-science and supramolecular chemistry in liquid-crystalline (LC) assemblies is expected to provide new soft materials with dynamic and anisotropic functions.[11–30] For example, development of supramolecular LC polymers has resulted in the induction of their stimuli-responsive and self-healing properties as well as facile and simple formation processes.[26–30]

Our strategy here is to develop hybrid supramolecular liquid crystals that exhibit polymer-like dynamic functions by the formation of rigid framework combining hydrogen bonds[31–36] and metal–ligand interactions[2,37–39] of low-molecular-weight compounds (Fig. 1). The combination of hydrogen bonding interactions and coordination chemistry has been reported for the preparation of non-LC dynamic polymers.[40,41] However, the number of metallomesogens based on complementary

hydrogen-bonded complexes is quite limited probably due to high melting temperatures for metallomesogens.[42–44]

Our intention is to use a forklike mesogenic ligand having pyridine moieties capable of both metal coordination and hydrogen bonds to produce metal-containing hydrogen-bonded supramolecular LC polymers and networks. Metal–ligand interactions between Ag$^+$ ions and pyridine moieties have been utilized to prepare supramolecular structures.[2,45–49] We previously reported that forklike pyridine-based ligands were self-assembled only with Pd^{2+} ions to construct giant discrete LC materials.[50] However, only discrete and closed structures were obtained by this approach.[50] Hybridization of coordination bonds and complementary hydrogen bonds based on pyridine moieties for the development of supramolecular LC materials remains unexplored.

LC elastomers exhibiting self-healing and shape memory properties are emerging class of smart polymer materials and have been extensively studied.[51–63] Tuning of mechanical and thermal properties of non-LC materials through molecular design was reported to be key to realize the macroscopic dynamic functions such as actuation, sensing, and self-healing properties.[64–70] However, conventional LC elastomers require covalently-bonded polymer backbones obtained by polymerization of reactive mesogens, which limits the design of LC elastomers.[4,5,52,53,62] If the self-assembly of low-molecular-weight compounds is employed as a new approach to prepare

Department of Chemistry and Biotechnology, School of Engineering, The University of Tokyo, Hongo, Bunkyo-ku, Tokyo 113-8656, Japan. E-mail: kato@chiral.t.u-tokyo.ac.jp; j_uchida@chembio.t.u-tokyo.ac.jp

† Electronic supplementary information (ESI) available. See DOI: 10.1039/d0sc06676a

‡ Current address: Research Center for Functional Materials, National Institute for Materials Science, Sengen, Tsukuba, Ibaraki 305-0047, Japan.
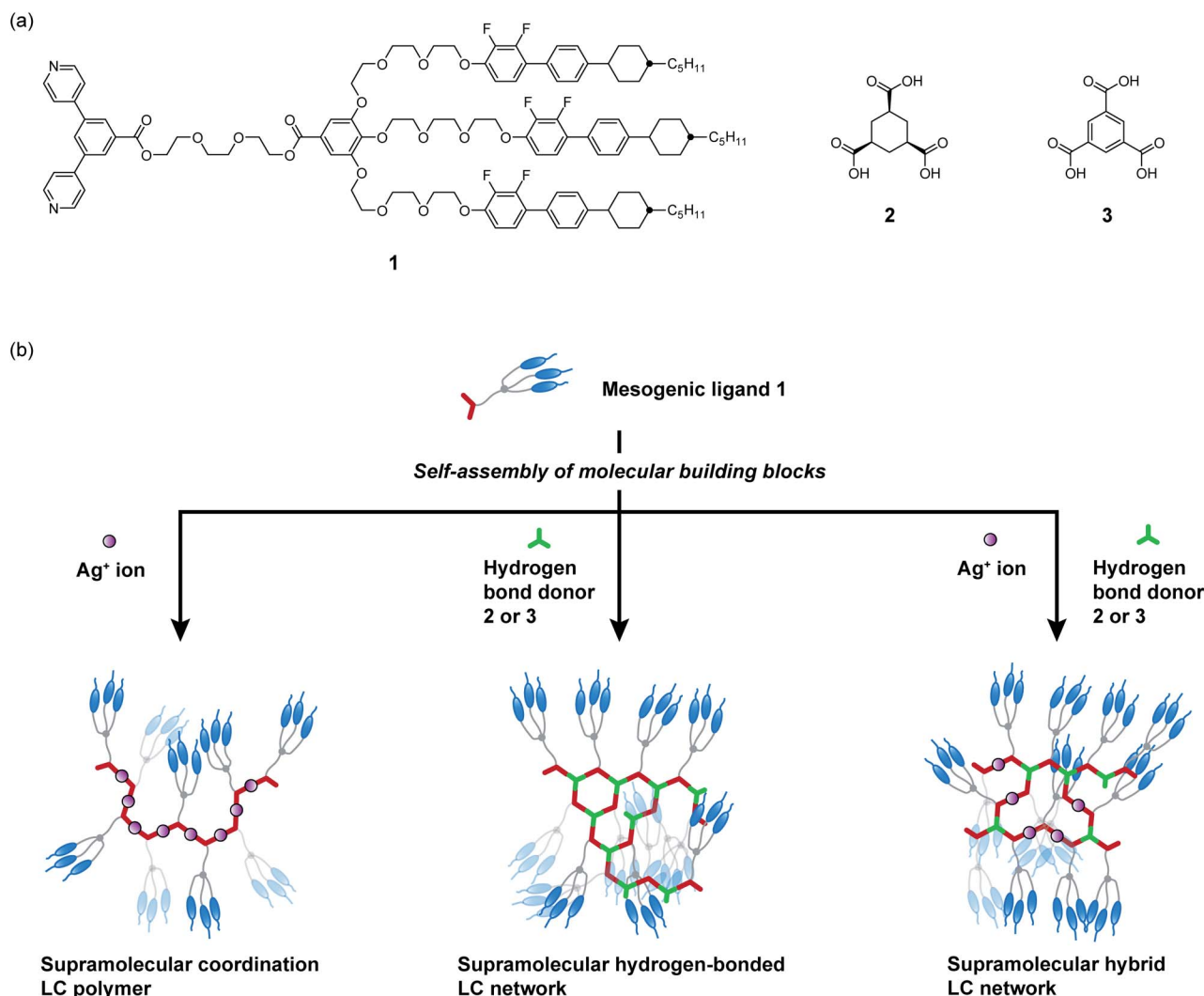
(a)

(b)

Fig. 1 (a) Molecular structures of 1–3. (b) Schematic illustration of material design for the development of self-healing and shape memory LC networks through hydrogen bonding and metal–ligand interactions of molecular building blocks.

supramolecular LC elastomers, nanostructured smart materials with tunable responsiveness would be easily obtained.

Here we report self-healing shape memory supramolecular LC polymers formed by self-assembly of pyridine-based forklike mesogenic ligand **1**, (1α,3α,5α)-1,3,5-cyclohexanetricarboxylic acid **2**, and **AgCF₃SO₃** (Fig. 1a). Free-standing and moldable supramolecular LC materials showing reversible thermotropic phase transitions were expected to be obtained by bottom-up synthesis of noncovalently crosslinked networks of small molecular components. The stimuli-responsive properties and phase transition behavior were intended to be tuned by changing the ratio of **2** and **AgCF₃SO₃** to **1**.

Results and discussion

Material design

We designed forklike ligand **1** by combining a bispyridyl ligand and rigid-rod mesogens (Fig. 1a).[50] The forklike mesogenic structures have been employed to induce LC properties for

supramolecular complexes.[50,71–74] We chose **AgCF₃SO₃** as the Ag⁺ source to build supramolecular coordination LC polymers because of the high thermal stability of the tri-fluoromethanesulfonate anion. The Ag⁺ cation usually forms a linear coordination geometry with pyridine-based ligands.[2,45–49,75] We considered that self-assembly of mesogenic ligand **1** and **AgCF₃SO₃** in a 1 : 1 molar ratio would produce side-chain supramolecular coordination LC polymer [**1**/**AgCF₃SO₃** (1 : 1)]. On the other hand, complexation of ligand **1** with cyclohexane-based tricarboxylic acid **2** in a 3 : 2 molar ratio would allow the formation of hydrogen-bonded supramolecular LC network **1**/**2** (3 : 2) because **1** is a bifunctional hydrogen bond acceptor and **2** is a trifunctional hydrogen bond donor. Benzene-based tricarboxylic acid **3**, which has similar geometry to **2**, was also chosen to compare their self-assembled properties. Furthermore, we envisioned that use of both hydrogen bonds and metal–ligand interactions for the construction of the hybrid networks consisting of **1**, **2**, and **AgCF₃SO₃** (**1**/**2**/**AgCF₃SO₃**) may lead to the development of new

stimuli-responsive supramolecular LC materials by tuning the ratio of these building blocks.

Supramolecular formation, processing and alignment control

LC complexes of $1/AgCF_3SO_3$ (1 : 1), $1/2$ (3 : 2), and $1/2/AgCF_3$-SO_3 (3 : 1.2 : 1.2) exhibiting homogeneous phases were successfully obtained by self-assembly of the molecular building blocks and Ag^+ ions. In contrast, macroscopic phase separation was observed for the 3 : 2 molar mixture of 1 and 1,3,5-benzenetricarboxylic acid 3 under optical microscopy. This behavior was caused by strong aggregation of compound 3 itself. Hydrogen-bonded network $1/2$ (3 : 2) and hybrid network $1/2/AgCF_3SO_3$ (3 : 1.2 : 1.2) showed free-standing and elastic properties as well as anisotropic LC molecular order. These materials can be processed into a variety of macroscopic shapes such as films (Fig. 2a) and strings (Fig. 2b) in the LC phases. The film of $1/2$ (3 : 2) was aligned by applying shear force in the LC phase. The 2D small-angle X-ray diffraction (XRD) measurement showed the split diffraction pattern (Fig. S1†). These results indicate that the mesogenic moieties were aligned perpendicular to the shearing direction in the film state. Furthermore, by
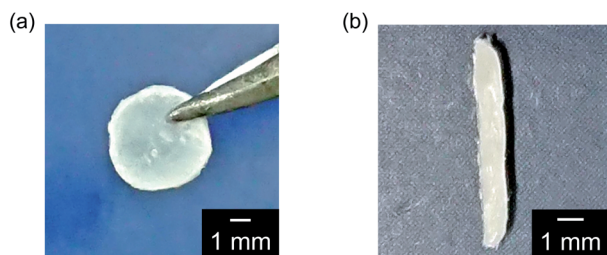

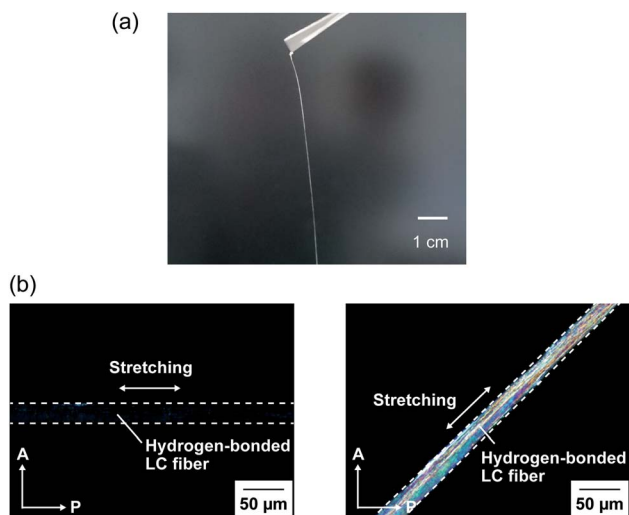Fig. 2 Photographs of hydrogen-bonded LC network $1/2$ (3 : 2): (a) film shape; (b) string shape.

Fig. 3 (a) Photograph of aligned supramolecular LC glassy fiber of $1/2$ (3 : 2). (b) Polarizing optical micrographs of the aligned LC fiber of $1/2$ (3 : 2). Directions of the analyzer (A), polarizer (P), and mechanical stretching are indicated with white arrows.

pulling from the isotropic melt and cooling, the unidirection-ally aligned supramolecular LC glassy fiber of $1/2$ (3 : 2) was obtained (Fig. 3). The periodic change of the birefringence was observed upon 45° rotation of the sample under crossed Nicols condition (Fig. 3b). Such polymer-like properties are unique for hydrogen-bonded LC materials formed by self-assembly of small molecular components based on single hydrogen bonding. On the other hand, no elastic properties were observed for simpler coordination polymer $1/AgCF_3SO_3$ (1 : 1) probably due to the strong intermolecular interactions.

Self-healing and shape memory properties

The free-standing and dynamic properties of the supramolec-ular LC networks enabled demonstration of self-healing behavior (Fig. 4 and S2†). Hydrogen-bonded network $1/2$ (3 : 2) and hybrid network $1/2/AgCF_3SO_3$ (3 : 1.2 : 1.2) both showed self-healing properties. For example, after attaching the two cut pieces of $1/2$ (3 : 2) and annealing at 100 °C in the LC phase for 30 minutes, adhesion of the two pieces was observed (Fig. 4). Dynamic nature of hydrogen bonds contributed to the self-healing properties of these supramolecular LC materials. Furthermore, we found that the self-healing properties of $1/2/$ $AgCF_3SO_3$ (3 : 1.2 : 1.2) were combined with shape memory effects (Fig. 5 and S3a†). After the procedure for self-healing experiments (photo II → III in Fig. 5), the string-shaped sample of $1/2/AgCF_3SO_3$ (3 : 1.2 : 1.2) was deformed at 60 °C in the LC phase (photo III → IV in Fig. 5). The deformed sample was rapidly cooled to room temperature under stress to form the glassy state, where the deformed shape was fixed as temporary shape (photo IV in Fig. 5). The temporary shape was
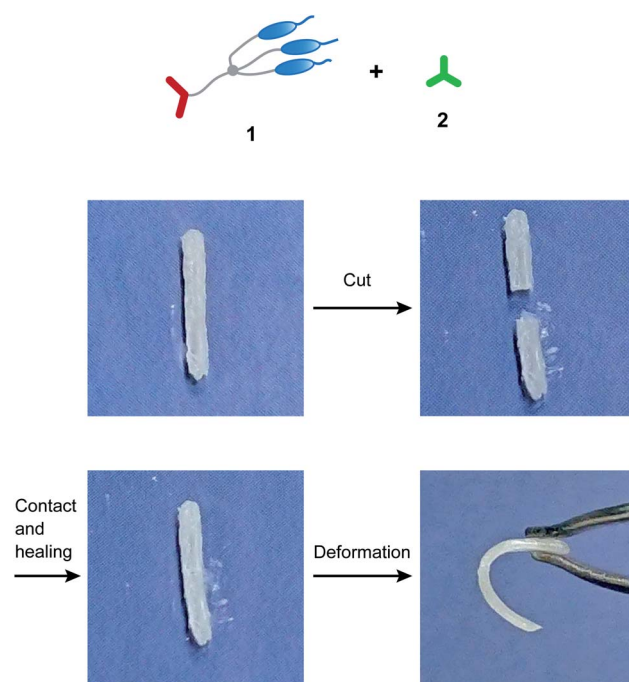

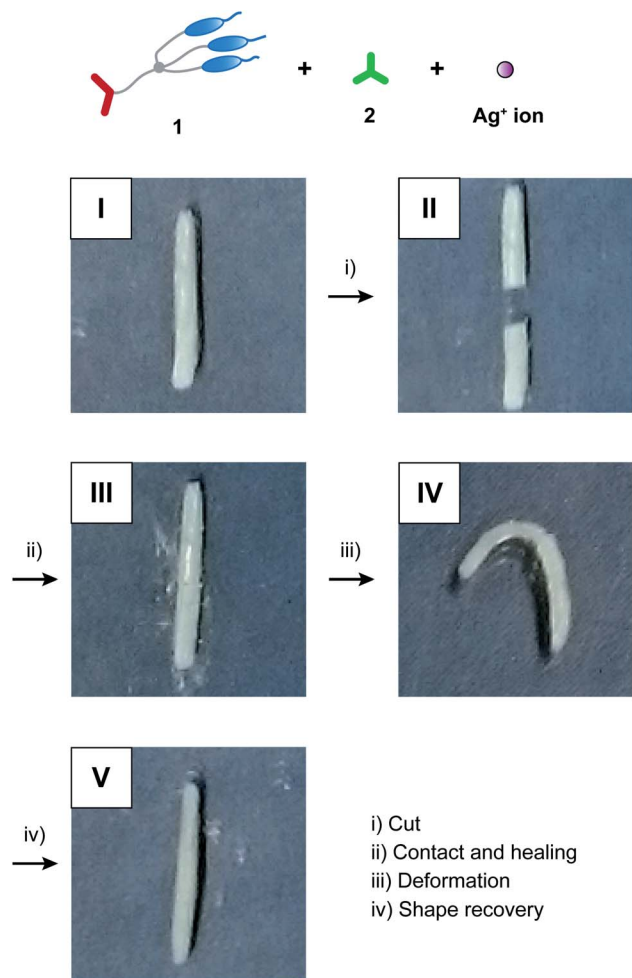Fig. 4 Self-healing behavior for hydrogen-bonded LC network $1/2$ (3 : 2).

Fig. 5 Self-healing and shape memory effects for hybrid LC network **1/2/AgCF₃SO₃** (3 : 1.2 : 1.2).

recovered to permanent string shape by heating to 60 °C within 30 seconds (photo IV → V in Fig. 5). In contrast, hydrogen-bonded network **1/2** (3 : 2) did not show sufficient recovery to permanent shape (Fig. S3†). This difference can be explained in terms of the strength of intermolecular interactions as follows. For the hybrid LC networks combining hydrogen bonds and coordination bonds, intermolecular interactions of supramolecular network structures may be enhanced through the incorporation of metal ions into the LC networks,[2] leading to the formation of ionic hard segments. Thus, the full shape recovery of the materials was achieved for the hybrid network of **1/2/AgCF₃SO₃** (3 : 1.2 : 1.2) probably due to entropy elasticity. The hydrogen-bonded network of **1/2** (3 : 2) was more dynamic than the hybrid network of **1/2/AgCF₃SO₃** (3 : 1.2 : 1.2) because of the absence of hard segments, and therefore it may be difficult to memorize the initial shape of **1/2** (3 : 2).

Supramolecular structure characterization

The structures of the supramolecular LC polymers and networks were examined by Fourier transform infrared (FT-IR) spectroscopy (Fig. 6 and S4†). The carbonyl peak of **2**
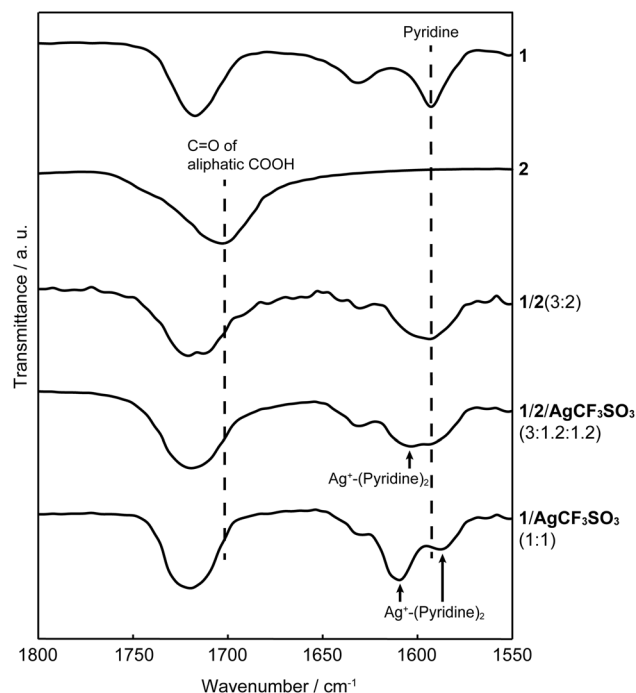

Fig. 6 FT-IR spectra of **1**, **2**, **1/2** (3 : 2), **1/2/AgCF₃SO₃** (3 : 1.2 : 1.2), and **1/AgCF₃SO₃** (1 : 1).

appeared at around 1700 cm⁻¹. For hydrogen-bonded network **1/2** (3 : 2), the carbonyl peak of **2** shifted to 1720 cm⁻¹ after complexation with **1**. The same shift of the carbonyl peak of **2** was observed for network **1/2/AgCF₃SO₃** in a 3 : 1.2 : 1.2 molar ratio. These observation can be explained by the formation of hydrogen-bonded complexes through the dissociation of carboxylic acid dimers into pyridine–carboxylic acid complexes.[76–78] Moreover, interactions between Ag⁺ ions and pyridine moieties were also suggested in **1/2/AgCF₃SO₃** (3 : 1.2 : 1.2) since a new peak appeared at 1605 cm⁻¹. The peak shift attributable to the metal–ligand interactions was more clearly observed for **1/AgCF₃SO₃** (1 : 1), which is consistent with a previous report on IR spectra of pyridine–Ag⁺ complexes.[79] These results indicate that hybrid supramolecular network **1/2/AgCF₃SO₃** (3 : 1.2 : 1.2) was constructed by self-assembly of small components through hydrogen bonds and metal–ligand interactions.

In order to study the formation of the polymeric structure of **1/AgCF₃SO₃** (1 : 1), ¹H NMR measurements of ligand **1** and **1/AgCF₃SO₃** (1 : 1) in CDCl₃ were performed (Fig. S5†). The signal of pyridine α protons showed downfield shift after complexation of ligand **1** with **AgCF₃SO₃**, which indicates the formation of coordination bonds between pyridine moieties and Ag⁺ ions. The broadened signals of **1/AgCF₃SO₃** (1 : 1) also suggest that large supramolecular structures with slow molecular motion were formed through metal–ligand interactions. Atomic force microscopy (AFM) observation was carried out to gain further insight into the structure of supramolecular coordination polymer **1/AgCF₃SO₃** (1 : 1) (Fig. S6†). The 2D and 3D AFM images of **1/AgCF₃SO₃** (1 : 1) showed the formation of fibrous aggregates (Fig. S6a and b†). The height profile of **1/AgCF₃SO₃**

(1 : 1) showed that the diameter of thinner fibers was 2–3 nm (Fig. S6c†). Although the estimated size of **1/AgCF$_3$SO$_3$** (1 : 1) was small considering the bulky mesogenic moieties, it was reported that side chains connected to the polymer backbones may not be fully extended on mica under AFM observation in air.[80,81] Based on these results, **1/AgCF$_3$SO$_3$** (1 : 1) was proposed to form a supramolecular coordination polymer having forklike mesogenic moieties in the side chain through self-assembly of ligand **1** and **AgCF$_3$SO$_3$**.

Liquid-crystalline properties

The supramolecular complexes of **1/2** (3 : 2), **1/2/AgCF$_3$SO$_3$** (3 : 1.6 : 0.6), **1/2/AgCF$_3$SO$_3$** (3 : 1.2 : 1.2), and **1/AgCF$_3$SO$_3$** (1 : 1) exhibited LC properties over wide temperature ranges (Fig. S7†). The phase transition properties of the supramolecular LC polymers and networks are summarized in Table 1. The complexation of ligand **1** with **2** and **AgCF$_3$SO$_3$** induced thermal stabilization of LC phases. Moreover, LC properties of the supramolecular networks were enhanced by the introduction of Ag$^+$ ions into the hydrogen-bonded LC network. The isotropization temperatures of the supramolecular complexes showed an increasing trend with the increase of the ratio of Ag$^+$ ions (Table 1). The supramolecular coordination LC polymer of **1/AgCF$_3$SO$_3$** (1 : 1) gradually decomposed above 190 °C and hence the LC-isotropic phase transition was not observed. The intermolecular interactions of polymer backbones may be enhanced by the addition of Ag$^+$ ions. These results are consistent with the shape memory behavior of hydrogen-bonded LC network **1/2** (3 : 2) and hybrid LC network **1/2/AgCF$_3$SO$_3$** (3 : 1.2 : 1.2).

Polarizing optical microscopy (POM) images of **1/2** (3 : 2) and **1/2/AgCF$_3$SO$_3$** (3 : 1.2 : 1.2) showed different alignment properties in the LC phases (Fig. 7a and b). The hydrogen-bonded LC network of **1/2** (3 : 2) formed homeotropic alignment in the LC phase on the glass substrate (Fig. 7a). Similar homeotropic alignment was previously reported for LC molecules composed of polar and nonpolar moieties.[71,73] On the other hand, the introduction of metal–ligand interactions into the hydrogen-bonded network partially disturbed the homeotropic alignment for hybrid LC network **1/2/AgCF$_3$SO$_3$** (3 : 1.2 : 1.2) (Fig. 7b) probably because of stronger intermolecular interactions and
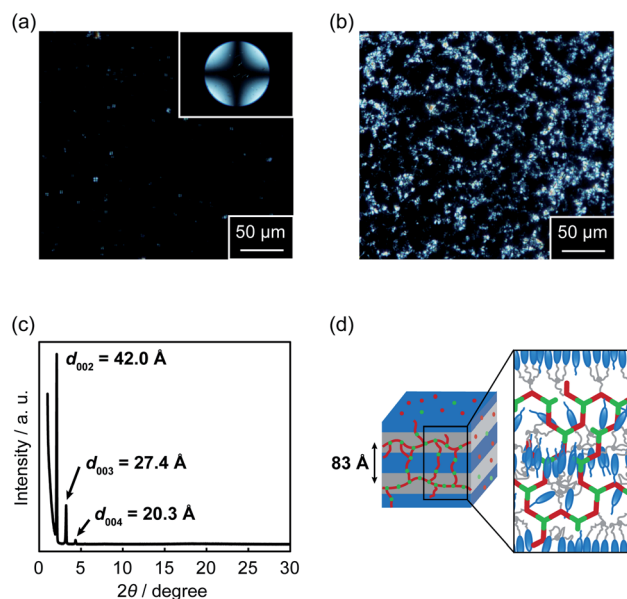
Fig. 7 Polarizing optical micrographs of (a) hydrogen-bonded LC network **1/2** (3 : 2) at 100 °C and (b) hybrid LC network **1/2/AgCF$_3$SO$_3$** (3 : 1.2 : 1.2) at 100 °C. The insert shows the conoscopic image. (c) X-ray diffraction pattern of **1/2** (3 : 2) at 100 °C. (d) A plausible assembled structure of **1/2** (3 : 2).

high viscosity of metal-containing liquid crystals. As for supramolecular coordination polymer **1/AgCF$_3$SO$_3$** (1 : 1), a polydomain texture was observed in a viscous fluid state under POM observation (Fig. S8†).

XRD measurements were carried out to examine the detailed assembled structures of the supramolecular LC polymers and networks. XRD pattern of complex **1/2** (3 : 2) at 100 °C gave several periodic peaks at 42.0, 27.4, and 20.3 Å (Fig. 7c), which were respectively assigned to the (002), (003), and (004) diffractions of a smectic A phase with the average spacing of 83 Å. This observation showed the formation of a bilayer structure of mesogenic moieties. A plausible assembled structure of complex **1/2** (3 : 2) in the LC phase is schematically shown in Fig. 7d. A similar smectic phase with the layer spacing of 81 Å was also formed for supramolecular coordination LC polymer **1/AgCF$_3$SO$_3$** (1 : 1) (Fig. S9†). In contrast to **1/2** (3 : 2) and **1/AgCF$_3$SO$_3$** (1 : 1), XRD pattern of hybrid LC network **1/2/AgCF$_3$SO$_3$** (3 : 1.2 : 1.2) showed not only several periodic peaks corresponding to a layered structure with the spacing of 77 Å but also a weak diffraction peak with a periodicity of 31 Å (Fig. S10†). This might be due to the formation of local order of network structures[82,83] in a smectic LC phase. These results suggest that the LC nanostructure of **1/2/AgCF$_3$SO$_3$** (3 : 1.2 : 1.2) was modulated by combining metal–ligand interactions with hydrogen bonds, leading to the macroscopic dynamic functions of supramolecular LC networks formed from small molecules and metal ions.

Conclusions

In conclusion, self-assembly of small molecular building blocks through hydrogen bonds and metal–ligand interactions leads to

Table 1 Phase transition temperatures of the supramolecular LC complexes and ligand **1**

Complex	Transition temperature[a,b]/°C				
1/2 (3 : 2)	Iso	151	SmA	34	G
1/2/AgCF$_3$SO$_3$ (3 : 1.6 : 0.6)	Iso	167	Sm	35	G
1/2/AgCF$_3$SO$_3$ (3 : 1.2 : 1.2)	Iso	174	Sm	35	G
1/AgCF$_3$SO$_3$ (1 : 1)	—[c]		SmA	35[d]	G
1[e]	Iso	106	SmA	15	G

[a] Transition temperatures (°C) were determined by differential scanning calorimetry (DSC) on the first cooling at the scanning rate of 10 °C min^{-1}. [b] Iso: isotropic; SmA: smectic A; Sm: unidentified smectic; G: glassy. [c] Thermal degradation occurred above 190 °C before isotropization. [d] Observed on the first cooling from 150 °C. [e] Ref. 50.

the formation of hybrid supramolecular LC networks exhibiting self-healing and shape memory properties. The combination of hydrogen bonding interactions and coordination bonds is key to achieve the macroscopic dynamic properties of free-standing and moldable supramolecular LC materials. Further complex mechanical responses can be realized by manipulating the alignment of the anisotropic LC networks.[4,5,51–56] The supramolecular approach presented here would provide a new material design for the development of smart LC materials and functional LC membranes based on self-assembly of low-molecular-weight compounds.

Experimental section

Preparation of the supramolecular LC complexes

The hydrogen-bonded LC networks were prepared by the evaporation technique. Typically, the THF solution containing the stoichiometric amount of ligand **1** and compound **2** was evaporated under reduced pressure. The resulting solids were dried *in vacuo* to give hydrogen-bonded LC networks. The supramolecular coordination LC polymers and hybrid LC networks were also prepared in a similar manner using the appropriate amount of the building blocks. For the observation of self-healing and shape memory effects, the string-shaped supramolecular LC materials with the dimension of around 7 mm in length and 1 mm in diameter were prepared.

Materials and characterization

All of the reagents were purchased from Tokyo Kasei, Aldrich, Kanto, and Wako. They were used without further purification. The FT-IR spectroscopy was conducted with a JASCO FT/IR-6100 Plus spectrometer and a JASCO IRT-5000 spectrometer with a LINKAM LTS350 hot stage. NMR spectra was recorded on a JEOL JNM-ECX400 (400 MHz) spectrometer. The chemical shifts of the ^{1}H NMR signals are referenced with respect to the internal standard Me_4Si ($\delta = 0.00$). AFM images were taken by Bruker Multimode 8 AFM with Nanoscope V controller. The samples for AFM observation were prepared by casting dilute $CHCl_3$ solution of **1**/$AgCF_3SO_3$ (1 : 1) at the concentration of 0.01 wt% on mica. The polarizing optical micrographs were recorded with an Olympus BX51 microscope equipped with a Mettler FP82HT hot stage. DSC measurements were performed with a NETZCH DSC 204 Phoenix system at the scanning rate of 10 °C min^{-1}. Wide-angle and small-angle XRD measurements were carried out with a Rigaku RINT-2500 diffractometer with a heating stage using Ni-filtered CuKα radiation.

Author contributions

T. K. and J. U. conceived and designed the project. T. K. and J. U. wrote the paper. J. U. performed the experiments. M. Y. designed a molecule. All authors read and commented on the manuscript.

Conflicts of interest

There are no conflicts to declare.

Acknowledgements

Notes and references

1 T. Kato, J. Uchida, T. Ichikawa and T. Sakamoto, *Angew. Chem., Int. Ed.*, 2018, **57**, 4355.

2 D. W. Bruce, *Acc. Chem. Res.*, 2000, **33**, 831.

3 T. Kato, *Struct. Bonding*, 2000, **96**, 95.

4 T. J. White and D. J. Broer, *Nat. Mater.*, 2015, **14**, 1087.

5 H. Yu and T. Ikeda, *Adv. Mater.*, 2011, **23**, 2149.

6 K. Ariga, T. Mori, T. Kitao and T. Uemura, *Adv. Mater.*, 2020, **32**, 1905657.

7 T. Kato, J. Uchida, T. Ichikawa and B. Soberats, *Polym. J.*, 2018, **50**, 149.

8 T. Kato, M. Gupta, D. Yamaguchi, K. P. Gan and M. Nakayama, *Bull. Chem. Soc. Jpn.*, 2021, **94**, 357.

9 J. W. Goodby, I. M. Saez, S. J. Cowling, V. Görtz, M. Draper, A. W. Hall, S. Sia, G. Cosquer, S.-E. Lee and E. P. Raynes, *Angew. Chem., Int. Ed.*, 2008, **47**, 2754.

10 R. Lan, J. Sun, C. Shen, R. Huang, L. Zhang and H. Yang, *Adv. Funct. Mater.*, 2019, **29**, 1900013.

11 T. Kato, M. Yoshio, T. Ichikawa, B. Soberats, H. Ohno and M. Funahashi, *Nat. Rev. Mater.*, 2017, **2**, 17001.

12 W. He, G. Pan, Z. Yang, D. Zhao, G. Niu, W. Huang, X. Yuan, J. Guo, H. Cao and H. Yang, *Adv. Mater.*, 2009, **21**, 2050.

13 J. Lugger, D. J. Mulder, R. Sijbesma and A. Schenning, *Materials*, 2018, **11**, 104.

14 S. J. Rowan and P. T. Mather, *Struct. Bonding*, 2008, **128**, 119.

15 D. W. Bruce, in *Supramolecular Chemistry: From Molecules to Nanomaterials*, ed. J. W. Steed and P. A. Gale, Wiley, Oxford, 2012, vol. 7, p. 3493.

16 F. Vera, J. L. Serrano and T. Sierra, *Chem. Soc. Rev.*, 2009, **38**, 781.

17 L. Chen, C. Chen, Y. Sun, S. Lu, H. Huo, T. Tan, A. Li, X. Li, G. Ungar, F. Liu and M. Zhang, *Angew. Chem., Int. Ed.*, 2020, **59**, 10143.

18 W. Li, Y. Kim and M. Lee, *Nanoscale*, 2013, **5**, 7711.

19 B. Therrien, *Inorganics*, 2020, **8**, 2.

20 R. J. Carlton, J. T. Hunter, D. S. Miller, R. Abbasi, P. C. Mushenheim, L. N. Tan and N. L. Abbott, *Liq. Cryst. Rev.*, 2013, **1**, 29.

21 A. Kuwabara, M. Enomoto, E. Hosono, K. Hamaguchi, T. Onuma, S. Kajiyama and T. Kato, *Chem. Sci.*, 2020, **11**, 10631.

22 S. Kawano, M. Kato, S. Soumiya, M. Nakaya, J. Onoe and K. Tanaka, *Angew. Chem., Int. Ed.*, 2018, **57**, 167.

23 K. V. Axenov and S. Laschat, *Materials*, 2011, **4**, 206.

24 R. Lan, J. Sun, C. Shen, R. Huang, Z. Zhang, L. Zhang, L. Wang and H. Yang, *Adv. Mater.*, 2020, **32**, 1906319.

25 R. Lan, J. Sun, C. Shen, R. Huang, Z. Zhang, C. Ma, J. Bao, L. Zhang, L. Wang, D. Yang and H. Yang, *Adv. Funct. Mater.*, 2020, **30**, 2000252.

26 D. J. Broer, C. M. W. Bastiaansen, M. G. Debije and A. P. H. J. Schenning, *Angew. Chem., Int. Ed.*, 2012, **51**, 7102.

27 T. Kato, H. Kihara, U. Kumar, T. Uryu and J. M. J. Fréchet, *Angew. Chem., Int. Ed. Engl.*, 1994, **33**, 1644.

28 A. H. Gelebart, D. J. Mulder, M. Varga, A. Konya, G. Vantomme, E. W. Meijer, R. L. B. Selinger and D. J. Broer, *Nature*, 2017, **546**, 632.

29 J. Mamiya, A. Yoshitake, M. Kondo, Y. Yu and T. Ikeda, *J. Mater. Chem.*, 2008, **18**, 63.

30 W. Hu, J. Sun, Q. Wang, L. Zhang, X. Yuan, F. Chen, K. Li, Z. Miao, D. Yang, H. Yu and H. Yang, *Adv. Funct. Mater.*, 2020, **30**, 2004610.

31 T. Kato and J. M. J. Fréchet, *J. Am. Chem. Soc.*, 1989, **111**, 8533.

32 X. H. Cheng and H. F. Gao, in *Hydrogen Bonded Supramolecular Materials. Lecture Notes in Chemistry*, ed. Z.-T. Li and L.-Z. Wu, Springer, Berlin, Heidelberg, 2015, vol. 88, p. 133.

33 C. Fouquey, J.-M. Lehn and A.-M. Levelut, *Adv. Mater.*, 1990, **2**, 254.

34 C. B. St. Pourcain and A. C. Griffin, *Macromolecules*, 1995, **28**, 4116.

35 H. Kihara, T. Kato, T. Uryu and J. M. J. Fréchet, *Chem. Mater.*, 1996, **8**, 961.

36 S. Sivakova and S. J. Rowan, *Chem. Commun.*, 2003, 2428.

37 *Metallomesogens: Synthesis, Properties, and Applications*, ed. J. L. Serrano, Wiley-VCH, Weinheim, 1996.

38 C. Piguet, J.-C. G. Bünzli, B. Donnio and D. Guillon, *Chem. Commun.*, 2006, 3755.

39 A. Pitto-Barry, N. P. E. Barry, V. Russo, B. Heinrich, B. Donnio, B. Therrien and R. Deschenaux, *J. Am. Chem. Soc.*, 2014, **136**, 17616.

40 S. Wang and M. W. Urban, *Nat. Rev. Mater.*, 2020, **5**, 562.

41 M. D. Hager, S. Bode, C. Weber and U. S. Schubert, *Prog. Polym. Sci.*, 2015, **49**, 3.

42 C. Domínguez, B. Heinrich, B. Donnio, S. Coco and P. Espinet, *Chem.–Eur. J.*, 2013, **19**, 5988.

43 S. Coco, E. Espinet, P. Espinet and I. Palape, *Dalton Trans.*, 2007, 3267.

44 A. B. Miguel-Coello, M. Bardají, S. Coco, B. Donnio, B. Heinrich and P. Espinet, *Inorg. Chem.*, 2014, **53**, 10893.

45 D. W. Bruce, D. A. Dunmar, E. Lalinde, P. Maitlis and P. Styring, *Nature*, 1986, **323**, 791.

46 H. Kihara and T. Kato, *Macromol. Rapid Commun.*, 1997, **18**, 281.

47 H.-J. Kim, W.-C. Zin and M. Lee, *J. Am. Chem. Soc.*, 2004, **126**, 7009.

48 R. Dobrawa and F. Würthner, *J. Polym. Sci., Part A: Polym. Chem.*, 2005, **43**, 4981.

49 T. Fukino, H. Joo, Y. Hisada, M. Obana, H. Yamagishi, T. Hikima, M. Takata, N. Fujita and T. Aida, *Science*, 2014, **344**, 499.

50 J. Uchida, M. Yoshio, S. Sato, H. Yokoyama, M. Fujita and T. Kato, *Angew. Chem., Int. Ed.*, 2017, **56**, 14085.

51 S. Krause, F. Zander, G. Bergmann, H. Brandt, H. Wertmer and H. Finkelmann, *C. R. Chim.*, 2009, **12**, 85.

52 C. Ohm, M. Brehmer and R. Zentel, *Adv. Mater.*, 2010, **22**, 3366.

53 K. Urayama, *React. Funct. Polym.*, 2013, **73**, 885.

54 E.-K. Fleischmann and R. Zentel, *Angew. Chem., Int. Ed.*, 2013, **52**, 8810.

55 M. Warner and E. M. Terentjev, *Liquid Crystals Elastomers (Revised Edition)*, Clarendon Press, London, UK, 2007.

56 Z. Wen, K. Yang and J.-M. Raquez, *Molecules*, 2020, **25**, 1241.

57 S. Chen, H. Yuan, H. Zhuo, S. Chen, H. Yang, Z. Ge and J. Liu, *J. Mater. Chem. C*, 2014, **2**, 4203.

58 P. Rastogi, J. Njuguna and B. Kandasubramanian, *Eur. Polym. J.*, 2019, **121**, 109287.

59 B. Ni, H.-L. Xie, J. Tang, H.-L. Zhang and E.-Q. Chen, *Chem. Commun.*, 2016, **52**, 10257.

60 K. A. Burke and P. T. Mather, *J. Mater. Chem.*, 2010, **20**, 3449.

61 S. Ahn, P. Deshmukh, M. Gopinadhan, C. O. Osuji and R. M. Kasi, *ACS Nano*, 2011, **5**, 3085.

62 K. M. Lee, T. J. Bunning and T. J. White, *Adv. Mater.*, 2012, **24**, 2839.

63 Y. Li, O. Rios, J. K. Keum, J. Chen and M. R. Kessler, *ACS Appl. Mater. Interfaces*, 2016, **8**, 15750.

64 A. Lendlein and S. Kelch, *Angew. Chem., Int. Ed.*, 2002, **41**, 2034.

65 C. Liu, H. Qin and P. T. Mather, *J. Mater. Chem.*, 2007, **17**, 1543.

66 Q. Zhao, H. J. Qi and T. Xie, *Prog. Polym. Sci.*, 2015, **49–50**, 79.

67 Z.-C. Jiang, Y.-Y. Xiao, Y. Kang, M. Pan, B.-J. Li and S. Zhang, *ACS Appl. Mater. Interfaces*, 2017, **9**, 20276.

68 R. Tepper, S. Bode, R. Geitner, M. Jäger, H. Görls, J. Vitz, B. Dietzek, M. Schmitt, J. Popp, M. D. Hager and U. S. Schubert, *Angew. Chem., Int. Ed.*, 2017, **56**, 4047.

69 Y. Yang and M. W. Urban, *Chem. Soc. Rev.*, 2013, **42**, 7446.

70 R. J. Wojtecki, M. A. Meador and S. J. Rowan, *Nat. Mater.*, 2011, **10**, 14.

71 J. Uchida and T. Kato, *Liq. Cryst.*, 2017, **44**, 1816.

72 I. Aprahamian, T. Yasuda, T. Ikeda, S. Saha, W. R. Dichtel, K. Isoda, T. Kato and J. F. Stoddart, *Angew. Chem., Int. Ed.*, 2007, **46**, 4675.

73 E. D. Baranoff, J. Voignier, T. Yasuda, V. Heitz, J.-P. Sauvage and T. Kato, *Angew. Chem., Int. Ed.*, 2007, **46**, 4680.

74 Y.-X. Hu, X. Hao, L. Xu, X. Xie, B. Xiong, Z. Hu, H. Sun, G.-Q. Yin, X. Li, H. Peng and H.-B. Yang, *J. Am. Chem. Soc.*, 2020, **142**, 6285.

75 A. N. Khlobystov, A. J. Blake, N. R. Champness, D. A. Lemenovskii, A. G. Majouga, N. V. Zyk and M. Schröder, *Coord. Chem. Rev.*, 2001, **222**, 155.

76 T. Kato, J. M. J. Fréchet, P. G. Wilson, T. Saito, T. Uryu, A. Fujishima, C. Jin and F. Kaneuchi, *Chem. Mater.*, 1993, **5**, 1094.

77 T. Kato, T. Uryu, F. Kaneuchi, C. Jin and J. M. J. Fréchet, *Liq. Cryst.*, 1993, **14**, 1311.

78 T. Kato, C. Jin, F. Kaneuchi and T. Uryu, *Bull. Chem. Soc. Jpn.*, 1993, **66**, 3581.

79 S. Chakraborty and O. Dopfer, *ChemPhysChem*, 2011, **12**, 1999.

80 E. Kasëmi, W. Zhuang, J. P. Rabe, K. Fischer, M. Schmidt, M. Colussi, H. Keul, D. Yi, H. Cölfen and A. D. Schlüter, *J. Am. Chem. Soc.*, 2006, **128**, 5091.

81 W. Zhuang, C. Ecker, G. A. Metselaar, A. E. Rowan, R. J. M. Nolte, P. Samorí and J. P. Rabe, *Macromolecules*, 2005, **38**, 473.

82 X. Feng, X. Ding and D. Jiang, *Chem. Soc. Rev.*, 2012, **41**, 6010.

83 Y. Miwa, K. Taira, J. Kurachi, T. Udagawa and S. Kutsumizu, *Nat. Commun.*, 2019, **10**, 1828.